Phase separation models for cuprate stripe arrays

R. S. Markiewicz and C. Kusko
Physics Department and Barnett Institute, Northeastern University, Boston, Massachusetts 02115
(Received 26 February 2001; revised manuscript received 9 July 2001; published 22 January 2002)

An electronic phase separation model provides a natural explanation for a large variety of experimental results in the cuprates, including evidence for both stripes and larger domains, and a termination of the phase separation in the slightly overdoped regime, when the average hole density equals that in the charged stripes. Several models are presented for charged stripes, showing how density waves, superconductivity, and strong correlations compete with quantum size effects (QSE's) in narrow stripes. The energy bands associated with the charged stripes develop in the middle of the Mott gap, and the splitting of these bands can be understood by considering the QSE on a single ladder.

DOI: 10.1103/PhysRevB.65.064520 PACS number(s): 74.20.Mn, 74.72.−h, 71.45.Lr, 74.50.+r

I. INTRODUCTION

Possible electronic phase separation (EPS) in the cuprates is often found in the form of stripe phases. Thus, neutron diffraction measurements find evidence for fluctuating stripe order in $La_{2-x}Sr_xCuO_4$ (LSCO) associated with incommensurate inelastic neutron scattering,[1] which can be transformed into long-range charged stripe order[2] by codoping with Nd or Eu. Similar incommensurate peaks are found in other cuprates, and long-range charge-ordered states are also found[3] in strongly underdoped samples of $YBa_2Cu_3O_{7-\delta}$ (YBCO), with stripes parallel to the chains, while at higher doping short-range stripe order is found at virtually all temperatures up to the pseudogap T^*. However, EPS can also manifest itself in the form of *larger domains*, particularly if the dopant ions are somewhat mobile and can follow the hole motion. These domains, long known in $La_2CuO_{4+\delta}$, may recently have been found in scanning tunneling microscope[4] (STM) and microwave[5] studies of $Bi_2Sr_2CaCu_2O_{8+\delta}$ (Bi2212). These domains, taken together with evidence for the termination of the antiferromagnetic (AFM) stripes at a fixed doping,[6] provide extremely strong support for a phase separation scenario in the cuprates.

At this point it is essential to better characterize the nature of the stripes, in particular the charged stripes, and to understand how their properties affect physical phenomena, in particular photoemission spectra.[7–11] While fluctuations[7,8] play an important role in the real cuprates, we have constructed ordered stripe arrays for which detailed tight-binding calculations are possible.[9] Such calculations can aid in elucidating the structure of the charged stripes, both for wide stripes—how the preferred hole density is stabilized—and for narrow stripes—how quantum size effects (QSE's) modify properties of the stripes. The present paper provides an extended analysis of these issues; some of these results were summarized recently.[12]

The paper is organized as follows. Section II enumerates key issues which must be addressed in any EPS model of stripes, including determination of the hole density on charged stripes. The charged stripes are probably stabilized by some competing order, either magnetic or paramagnetic (including charge density waves). Section III shows that magnetic charged stripes can arise in a mean-field Hubbard model and can be either ferromagnetic or a linear antiferromagnetic (LAF) phase similar to the White-Scalapino stripes.[13] Calculations on stripe arrays find that the charged stripes lead to midgap states near the Fermi level. Section IV shows how these data can be interpreted in terms of QSE's on single stripes. Section V presents the results of single-stripe calculations: competing charge-density-wave (CDW) and superconducting orders can exist in paramagnetic stripes, but they are strongly modified by the QSE's. On LAF stripes, *d*-wave superconductivity and an unusual form of CDW's are both found to persist down to the narrowest (two cells wide) stripes. Section VI includes results on stripe arrays: the LAF stripes produce photoemission constant-energy maps in significantly better agreement with experiment. In the Discussion, Sec. VII, we summarize the reasons for our choice of the doping on the charge stripe, $x_0 \simeq 0.25$, and show that this provides a consistent picture explaining the termination of the AFM stripes slightly beyond optimal doping, the 1/8 anomaly, and the presence of domains at higher doping levels (including the Yamada plot). Further, we summarize evidence that superconductivity ''lives'' in the charged stripes. Conclusions are given in Sec. VIII.

II. KEY ISSUES FOR AN EPS MODEL OF STRIPES

A. Hole doping on charged stripes

A phase separation model of stripes is characterized by the two well-defined stable end phases between which phase separation takes place. The insulating stripes are generally understood to be AFM—essentially the same as the Mott insulator found in undoped cuprates. The hole-doped stripes are assumed to have a finite doping x_0. This simple idea has three experimentally verifiable characteristic features: (i) *the stripe phase must terminate* when $x = x_0$; (ii) there will be a *crossover* at a lower doping, $x_{cr} \sim x_0/2$, from magnetic-dominated ($x < x_{cr}$) to charge-dominated ($x > x_{cr}$) stripe arrays; and (iii) some *interaction* on the charged stripes stabilizes the end phase at x_0. In this paper, it will be assumed that $x_0 \simeq 0.25$, so the crossover x_{cr} corresponds to the 1/8 anomaly. In the Discussion, Sec. VII A, it will be demonstrated that this simple choice can consistently explain a large variety of data. It should be cautioned that while the present paper is written in terms of a smooth evolution of

stripe periodicity with doping, experimental data (e.g., the Yamada plot) are suggestive of commensurability pinning and the presence of EPS domains rather than stripes for $x > x_{cr}$.

B. What stabilizes charged stripes?

In any phase separation model, a key issue is understanding the nature of the charged stripes. Indeed, since superconductivity seems to arise predominantly in these stripes (Sec. VII B), such understanding is likely to play an important role in elucidating the origin of the high superconducting transition temperatures. For the stripe phase to exist, the doping x_0 must be particularly *stable*. This can arise via an electronic *instability*, which opens up a gap over much of the Fermi surface, making the electronic phase nearly incompressible. This ''stability from instability'' is a fairly general feature, underlying, e.g., Hume-Rothery alloys.[14] (This is a modification of an argument due to Anderson[15].) Here, we explore a number of candidates for the predominant electronic instability.

In a related paper,[16] we will provide strong evidence that this ''hidden order'' is a form of CDW's, which could include the flux phase. However, here we will explore a wider variety of possibilities. One issue is that in the low doping limit the charge stripes act as antiphase boundaries (APB's) for the AFM stripes. Such an effect arises naturally if the charged stripes have some residual magnetic interaction, and we will explore this possibility. However, in nickelates charged stripes coupled to a CDW are found to act as APB's.[17] The large Hubbard on-site repulsion U plays an important role. Strong correlation effects lead to two classes of charged stripe phases: either the constraint against double occupancy leads to magnetic order (magnetic charged stripes) or kinetic energy dominates, leading to a magnetically disordered phase (paramagnetic charged stripes) with reduced hopping, as in *t-j* (Ref. 18) and slave boson[19] models. Section III will provide examples of both classes, denoted as class B and class A stripes, respectively. Class A stripes could be simply correlated metals (as in *t-j* or slave boson calculations) or could have additional, e.g., CDW, order. A crossover from magnetic to correlated paramagnetic groundstate arises as a function of doping in models of itinerant ferromagnets.[20]

In the next section, we show that class B (magnetic) charge stripes can arise in a mean-field Hubbard model,[21] with the charged stripes displaying either ferromagnetic (FM) or LAF [ordering vector $(\pi,0)$] order. The LAF stripes are very similar to White-Scalapino (WS) stripes.[13] The FM phase is stabilized by VHS nesting; it may be present in ruthenates,[22] but is unlikely to be relevant for the cuprates (for one thing, the FM stripes are likely to be diagonal, and do not form APB's,[23] contrary to experiment). We have suggested that other VHS-stabilized phases are more likely[24] (see also Ref. 25), and here we explore the properties of a class A CDW phase.[19] At a doping $x \sim 0.25$, the effects of correlations are relatively weak, renormalizing the bandwidth by a factor of ~ 2. Thus, for the present calculations on paramagnetic stripes, it will be assumed that renormalized parameters are used, and other effects of strong correlations will be neglected.

While LAF stripes are most stable when $t' = 0$, we explore the possibility that they can be stabilized even when $t' \neq 0$ by on-stripe CDW or superconducting order. Ordinarily, the CDW phase is believed to *compete* with strong correlation effects, but we find (Sec. V B) that an unusual form of CDW phase can *coexist* with LAF order: the charge density varies between zero and one (not two) holes per atom.

C. Notation of stripes

In a stripe array, the alternating stripes are associated with the two stable thermodynamic phases. Here, we summarize the different ways these stripes are denoted in this paper. The stripe with lower hole doping is variously referred to as ''insulating'' or ''antiferromagnetic.'' (These are also known as magnetic stripes, since the charged stripes have considerably weaker magnetic order, but we will avoid that notation here.) The stripe with higher hole doping is generically referred to as ''charged'' or ''hole-doped.'' At low temperatures, these stripes are also ''superconducting,'' but at high temperatures, they are stabilized by some ''hidden order,'' and one purpose of this paper is to explore a number of possible orders. The orders fall into two groups: ''magnetic charged'' (class B) stripes could have FM or LAF order (the latter are White-Scalapino-like stripes), while ''paramagnetic'' (class A) stripes could have CDW or flux-phase order.

III. PHASE SEPARATION IN A MEAN-FIELD HUBBARD MODEL

Strong-coupling models would seem to be natural for producing phase-separated or striped ground states. Any magnetic ordering avoids double occupancy, while changing from one form of magnetic order to another, via, e.g., doping, requires highly collective spin rotations, as competing orders are orthogonal. While superexchange leads to AFM insulators at half filling, doping tends to favor textures with parallel spins (e.g., FM) to maximize hole hopping. Such ferron phases were introduced long before high T_c,[26] but it remains controversial whether such states are ground states of the Hubbard model.[27] While the *t-j* model does have phase separation for large J/t, it is unclear whether such phases extend to the values $J/t \sim 0.3$ expected for the cuprates.[13,28–30]

We have found phase-separated solutions of the Hubbard model at the mean-field level.[21] While these solutions are metastable in UHF calculations, they closely resemble the WS stripes, and provide an interesting example of phase-separation-mediated stripe phases. We find a well-defined surface tension for wide, isolated stripes, which decreases and changes sign as the stripes become narrower. When the surface tension becomes negative, the stripes no longer remain straight, and spontaneously meandering solutions are found.

These solutions are found by considering only low-order

commensurate phases, with wave vector $q_x, q_y \sim 0$ or $Q_i = \pi/a$ only. The bare dispersion is

$$\epsilon_k = -2t(c_x + c_y) - 4t' c_x c_y, \tag{1}$$

with $c_i = \cos k_i a$. The Hubbard interaction $U\Sigma_i (n_{i\uparrow} - 1/2)(n_{i\downarrow} - 1/2)$ leads to magnetic order with a mean-field magnetization m_q at wave vector $\vec{q}$, and the quasiparticle dispersion becomes

$$E_\pm = \epsilon_+ \pm E_0, \tag{2}$$

where

$$E_0 = \sqrt{\epsilon_-^2 + U^2 m_q^2} \tag{3}$$

and

$$\epsilon_\pm = \frac{1}{2}(\epsilon_k \pm \epsilon_{k+q}). \tag{4}$$

For the cuprates, we expect[9] $t \simeq 325$ meV, $U/t \simeq 6$, and $t'/t \simeq -0.276$. The magnetization is found self-consistently from

$$m_q = \sum_k [f(E_-) - f(E_+)] \frac{U m_q}{2E_0}, \tag{5}$$

with Fermi function $f(E) = 1/(1 + e^{(E - E_F)/k_B T})$. The resulting free energy is

$$F = E_q - TS + U\left(m_q^2 + \frac{x^2}{4}\right), \tag{6}$$

with

$$E_q = \sum_{k, i = \pm} E_i f(E_i), \tag{7}$$

$$S = k_B \sum_{k, i = \pm} \{f(E_i)\ln[f(E_i)] + [1 - f(E_i)]\ln[1 - f(E_i)]\}. \tag{8}$$

The competing phases include AFM for $\vec{q} = \vec{Q} \equiv (\pi, \pi)$, FM with $\vec{q} = (0,0)$, and LAF with $\vec{q} = (\pi, 0)$. When the LAF stripes are two cells wide, this LAF phase closely resembles the White-Scalapino stripes [Fig. 14(e) below]. The AFM state has the lowest free energy at half filling, but (for $t' = 0$) is unstable for finite hole doping. For $t' = 0$, there is phase separation between the AFM and LAF phases, while for finite t' the phase separation is between AFM and FM phases, Fig. 1. (When electron-phonon coupling is included, it is found that the FM phase is unstable with respect to a CDW phase.[16])

The LAF stripes for $t' = 0$ are discussed in Ref. 21. For $t' \neq 0$ electron-hole symmetry is absent; for hole doping $x > 0$, there is phase separation to a FM phase, consistent with recent simulations by Vozmediano *et al.*,[23] who find a uniform FM phase at $x = 0.15$ for $U = 8t, t' = 0.3t$. However, *on the electron-doped side a uniform AFM phase is stable over a large doping range*, suggestive of the asymmetry found in the cuprates. The dot-dashed curve in Fig. 1 shows that in the phase separation regime, the low-energy physics can be approximated by the form of free energy assumed in Ref. 9,

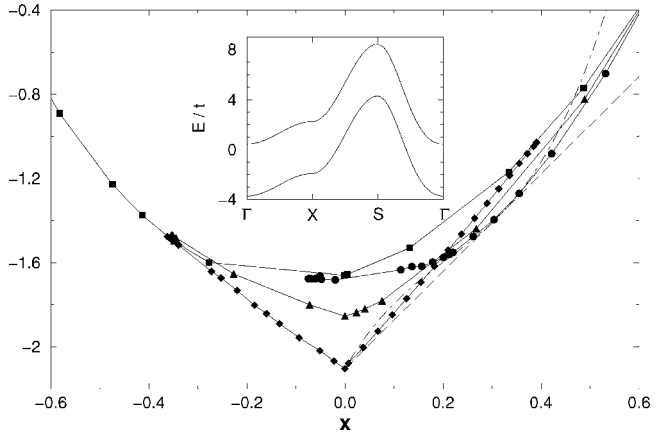

FIG. 1. Free energy vs doping for several magnetic phases of the Hubbard model assuming $U = 6.03t$ and $t' = -0.276t$. Diamonds = AFM, triangles = LAF, circles = FM, and squares = PM phase. Dashed lines = tangent construction; dot-dashed line = Eq. (9). Inset: dispersion of the FM phase at $x = 0.31$; Brillouin zone points $\Gamma = (0,0), X = (\pi, 0), S = (\pi, \pi)$.

$$f(x) = f_0 x\left(1 - \frac{x}{x_0}\right)^2 \tag{9}$$

(neglecting a term linear in x), with x_0 the hole doping of the uniform charged phase. The FM phase is stabilized by VHS nesting (inset to Fig. 1) as found previously.[22] The tangent construction tends to select the FM phase at dopings somewhat away from optimal nesting (Fermi energy above midgap). Both regimes of phase separation seem to be driven by hole delocalization: one dimensional (along the LAF rows) when $t' = 0$, two dimensional for finite t'.

The resulting phase diagrams x vs U, Fig. 2, are strikingly different. For $t' = 0$, Fig. 2(a), the phase separation is between the AFM and paramagnetic (LAF) phase for $U < U_c$

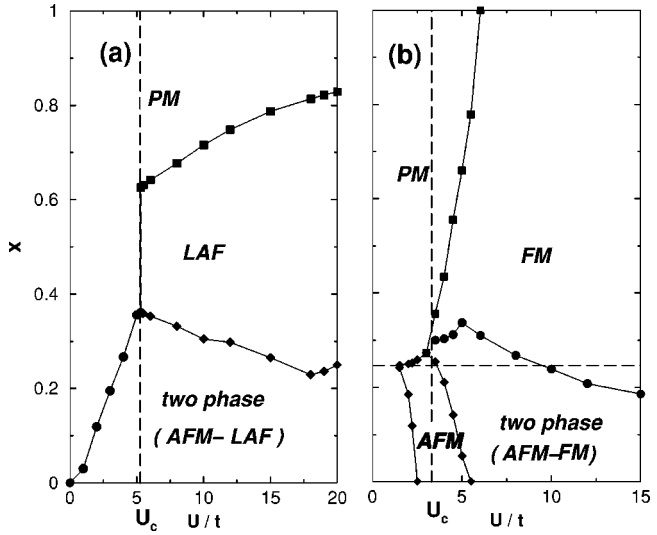

FIG. 2. Phase diagrams, $x(U)$ for the Hubbard model, with $t' = 0$ (a) or $t' = -0.276t$ (b). [Dashed line in (b) =doping of VHS.]

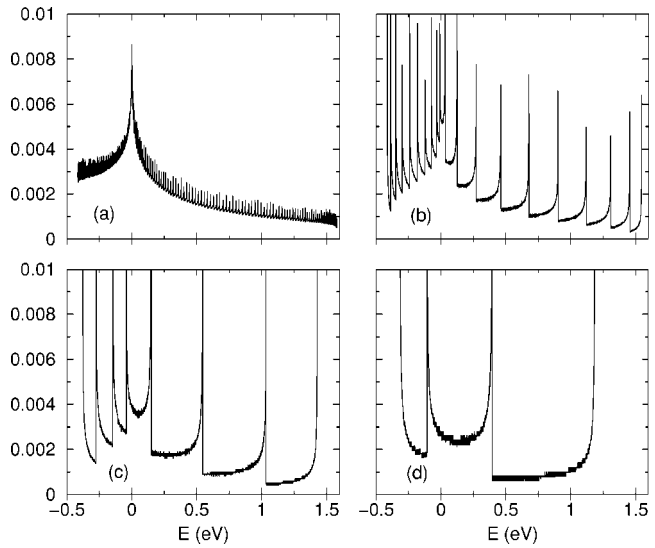

FIG. 3. Density of states for a single stripe of width $N=100$ (a), 10 (b), 4 (c), or 2 (d) atoms. Based on Eq. (1) with $t'/t=-0.276$.

$=5.3t$ ($U>U_c$), while for finite t', Fig. 2(b), there is generally a VHS-stabilized FM phase. For small U and $t'\neq 0$, there is a regime where simple spin-density-wave theory works and a uniform AFM phase is stable, but when $t'=0$ phase separation persists for all finite U. Note that U_c marks a crossover between class A (paramagnetic) and class B (magnetic) charged stripes. The value U_c is close to the $U=6.03t$ expected in the cuprates, although for finite t', U_c decreases, $U_c\sim 3t$ for $t'=-0.276t$, and the range of U for which paramagnetic stripes are stable becomes very small. While these stripes are metastable in UHF calculations, we will show below that the stability of phase separating stripes can be enhanced by *additional interactions* beyond the pure Hubbard model.

IV. ISOLATED STRIPES VS ARRAYS

In ordered stripe arrays it is found[9] that the AFM stripes have a Mott-Hubbard gap, and the features near the Fermi level are associated with the charged stripes. This charge stripe dispersion shows a series of quasi-one-dimensional features which qualitatively resemble the bands of an isolated stripe produced by QSE's. In this section, we make a quantitative comparison with isolated stripes and explore the mechanism of QSE-induced Van Hove splitting.

For a single stripe N Cu atoms wide, the dispersion is still given by Eq. (1), but the allowed k_x values are quantized, with $k_x=k_m\equiv m\pi/(N+1)$, $m=1,2,\ldots,N$. These are in fact the usual quantized Bloch bands, but for large N the quantization is not noticeable. For small N, the dispersion appears as a series of N overlapping one-dimensional (1D) dispersions. Equation (1) can be rewritten as N 1D dispersions

$$\epsilon_{m,k_y}=-2tc_m-2(t+2t'c_m)c_y. \tag{10}$$

These are the QSE's, with the corresponding density of states (DOS) shown in Fig. 3. Notice that for $N=100$, the VHS is readily apparent in the dispersion. Even down to $N=2$, the

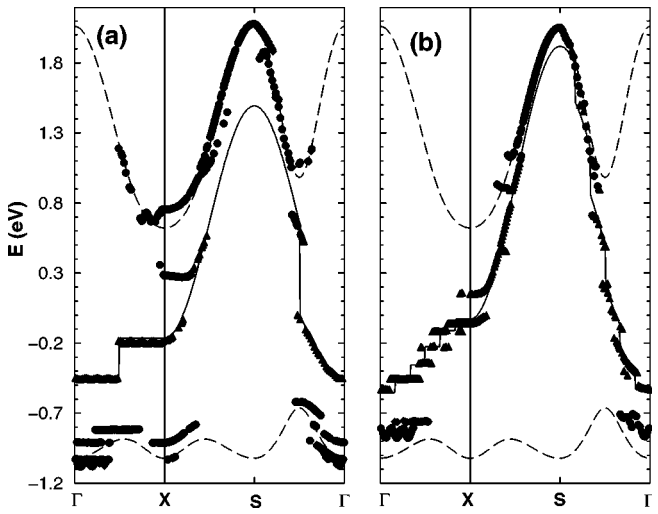

FIG. 4. Dispersion of stripe arrays: (a) (6,2) array with charged stripes two Cu wide (AFM stripes six Cu wide); (b) (2,6) array with charged stripes six Cu wide (AFM stripes two Cu wide). Data from Figs. 7(a) and 7(d), respectively, of Ref. 9; triangles (diamonds) = predominantly from charged (AFM) stripes, while circles = mixed origin; dashed line = Mott bands of AFM stripes; solid line = single (charged) stripe model, with k_x approximated by nearest quantized value.

VHS is clearly defined (albeit only within a finite interval) as the *locus of energies where all subbands overlap*. In fact, *the QSE opens a gap at the VHS*, effectively lowering the kinetic energy of the electrons just like a conventional (e.g., CDW) gap. The VHS splitting can be found from Eq. (10):

$$\Delta E_{VHS}=\epsilon_1^{max}-\epsilon_N^{min}=4t(1-c_1). \tag{11}$$

This splitting has two consequences: first, the VHS splitting enhances the stabilization of the striped phase, but second, the QSE gap competes with other gaps, such as CDW's and superconductivity. However, while the QSE splits the VHS peak, a substantial DOS remains ungapped, so additional instabilities remain possible. This competition will be discussed further in the next section.

It should be noted that this is the first direct demonstration that the VHS can be defined on a stripe only two atoms wide. The definition is quite analogous to the standard definition in two dimensions: the point at which the bands cross over from electron like to hole like.

Figure 4 compares the gaps of a single stripe with those found in the ordered stripe array;[9] the array is labeled (m,n) when the magnetic stripes are m coppers wide and the charged stripes are n coppers wide. In the array calculation, no competing order was introduced on the charged stripes, so the QSE provides the only gap. Figure 4 shows that there is a very good match for both two-Cu-wide and six-Cu-wide stripes, although for the two-Cu-wide stripe, the VHS gap is somewhat larger for the single stripe than in the array. From Eq. (10), the 1D bands have DOS peaks at the band bottom and top; the band bottom corresponds to $k_y=0$—i.e., the dispersion from $\Gamma\rightarrow X$ is flat, at the energy corresponding to the lower DOS peak. (The intensity along $\Gamma\rightarrow X$ is given by

a structure factor, which does not directly come into a single stripe calculation.) Along $X \rightarrow S$ one should see the 1D dispersion extrapolating to the band top at $S=(\pi,\pi)$. Given the good agreement, it should be possible to analyze competing orders on a single stripe, for which the calculations are simpler (no need to self-consistently adjust doping on each row to account for charging effects).

V. ORDERING ON SINGLE CHARGED STRIPES

A. CDW's and superconductivity on paramagnetic stripes

1. Electron-phonon coupling

In this section, we will develop two closely related models of the competition of CDW order and superconductivity *on a single charged stripe*. The first is a class A paramagnetic stripe, stabilized by electron-phonon coupling,[31,32] while the second has dominant electron-electron coupling, with (class B) magnetic charged stripe order.

An earlier calculation[31] used a Van Hove–stabilized CDW model to describe the doping dependence of the pseudogap. Here we reapply the model for a single stripe, by introducing the following modifications. (1) The calculation is carried out on a single, finite-width stripe. (2) Pinning to the VHS arises naturally, since all stripes are at the same doping. (3) For closer approximation to experiment, *d*-wave superconductivity is assumed. (4) Correlation effects due to the Hubbard U are neglected: previous slave boson calculations suggest that the main effect is a bandwidth renormalization by a factor ~ 2.[19]

We briefly recall the energy dispersion and the gap equations of the model,[31] generalized to *d*-wave superconductivity. In terms of a function

$$\Theta_{\vec{k}}=\begin{cases}1, & \text{if} \quad |\epsilon_{\vec{k}}-\epsilon_F|<\hbar\omega_{ph},\\ 0, & \text{otherwise,}\end{cases} \tag{12}$$

the gap functions are $\Delta_{\vec{k}}=\Delta_0\Theta_{\vec{k}}(c_x-c_y)/2$ for superconductivity and $G_{\vec{k}}=G_0+G_1\Theta_{\vec{k}}\Theta_{\vec{k}+\vec{Q}}$ for the CDW. The energy eigenvalues are $E_{\pm,k}$ and their negatives, with

$$E^2_{\pm,k}=\frac{1}{2}(E^2_k+E^2_{k+Q}+2G^2_k\pm\hat{E}^2_k), \tag{13}$$

$E^2_k=\epsilon^2_k+\Delta^2_k$, $\hat{E}^4_k=(E^2_k-E^2_{k+Q})^2+4G^2_k\tilde{E}^2_k$, $\tilde{E}^2_k=\epsilon^2_{k+}+(\Delta_k-\Delta_{k+Q})^2$, $\epsilon_{k\pm}=\epsilon_k\pm\epsilon_{k+Q}$, and the nesting vector $Q=(\pi,\pi)$. The gap equations are

$$\begin{aligned}\Delta=\lambda_\Delta\Delta\Sigma_{\vec{k}}&\frac{\Theta_{\vec{k}}(c_x-c_y)^2/4}{E^2_{+,k}-E^2_{-,k}}\\ &\times\left(\frac{E^2_{+,k}-\epsilon^2_{\vec{k}+\vec{Q}}-\Theta_{\vec{k}+\vec{Q}}[\Delta^2_{\vec{k}}+G^2_{\vec{k}}]}{2E_{+,k}}\tanh\frac{E_{+,k}}{2k_BT}\right.\\ &\left.-\frac{E^2_{-,k}-\epsilon^2_{\vec{k}+\vec{Q}}-\Theta_{\vec{k}+\vec{Q}}[\Delta^2_{\vec{k}}+G^2_{\vec{k}}]}{2E_{-,k}}\tanh\frac{E_{-,k}}{2k_BT}\right),\end{aligned} \tag{14}$$

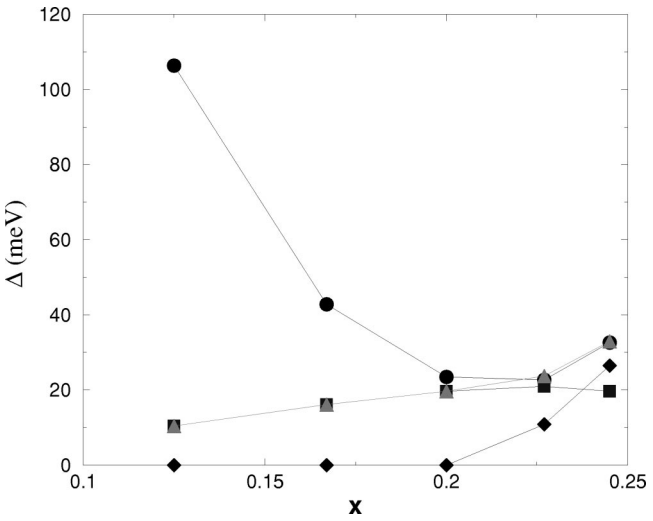

FIG. 5. Gaps in a paramagnetic stripe, as a function of doping (equivalently: stripe width), assuming $x_0=0.25, \lambda_{CDW}=0.5$ eV, $\lambda_\Delta=0.25$ eV. Squares = *s*-wave superconducting gap; diamonds = CDW gap; triangles = combined gap; circles = total gap at $(\pi,0)$, including the quantum confinement gap.

$$\begin{aligned}G_i=\lambda_G\Sigma_{\vec{k}}&\frac{\Theta_i G_{\vec{k}}}{E^2_{+,k}-E^2_{-,k}}\\ &\times\left(\frac{E^2_{+,k}+\epsilon_{\vec{k}}\epsilon_{\vec{k}+\vec{Q}}-\Delta^2_{\vec{k}}-G^2_{\vec{k}}}{2E_{+,k}}\tanh\frac{E_{+,k}}{2k_BT}\right.\\ &\left.-\frac{E^2_{-,k}+\epsilon_{\vec{k}}\epsilon_{\vec{k}+\vec{Q}}-\Delta^2_{\vec{k}}-G^2_{\vec{k}}}{2E_{-,k}}\tanh\frac{E_{-,k}}{2k_BT}\right),\end{aligned} \tag{15}$$

with interaction energies λ_Δ and λ_G, and $\Theta_0=\Theta_{\vec{k}}\Theta_{\vec{k}+\vec{Q}}$, $\Theta_1=1$.

The CDW-superconducting competition was studied in bulk in Ref. 31. The previous results are recovered for a sufficiently wide stripe (~ 100 Cu wide). For narrower stripes, it is found that the quantum confinement gap severely interferes with alternative gap formation. Figure 5 illustrates how the various gaps vary with stripe width, near $x_0=0.25$. The data are plotted versus average doping, assuming a regular stripe array with two-Cu-wide AFM stripes (which do not contribute to the gaps) and N-Cu-wide charged stripes of doping x_0, giving an average hole doping $x=Nx_0/(N+2)$.

The CDW gap is most sensitive to stripe width, but in the narrowest stripes superconductivity is also suppressed (the suppression is stronger for a *d*-wave gap). Strong instabilities are possible in the stripes, but they are shifted in doping away from $x_0=0.25$. Thus, the CDW instability requires both $E_{\vec{k}}$ and $E_{\vec{K}+\vec{Q}}$ to be near the Fermi level; for a two-cell-wide stripe, this is only possible near $x=0$. On the other hand, superconductivity is possible anywhere if the coupling is strong enough. For a two-cell-wide stripe, the optimal superconductivity arises when the Fermi level is at the *one-dimensional VHS* at the edge of one of the stripe subbands. This depends on t', and for $t'=-0.276t$ falls at $x=0.582$ (a larger gap is found on the electron-doped side, $x=-0.376$). It should be noted that, even though the superconductivity is

assumed to be *d*-wave, in general a finite minimum gap is found in the stripe, even when the CDW gap is zero. This is because the vanishing *d*-wave gap can be sampled only when the point $(\pi/2,\pi/2)$ is sufficiently close to the Fermi surface, which in general requires N to be odd [recall that the allowed values of k_x are integer multiples of $\pi/(N+1)$] or very large.

2. Electron-electron coupling

In the above calculations, the λ's arose from electron-phonon coupling.[32] Similar contributions follow from electron-electron coupling, in an extended Hubbard model. For instance, the near-neighbor Coulomb repulsion has the following mean-field expansion:

$$V\sum_{\langle i,j\rangle,\sigma,\sigma'} n_{i,\sigma}n_{j,\sigma'} = 4V\sum_{\vec{k},\sigma} c^{\dagger}_{\vec{k},\sigma}c_{\vec{k},\sigma} - 2V\langle O_n\rangle\sum_{\vec{k},\sigma}(c_x+c_y)c^{\dagger}_{\vec{k},\sigma}c_{\vec{k},\sigma} - 8V\langle T_x\rangle\sum_{\vec{k},\sigma} c^{\dagger}_{\vec{k}+\vec{Q},\sigma}c_{\vec{k},\sigma}$$
$$-4V\langle T_y\rangle\sum_{\vec{k},\sigma}\tilde{\gamma}_k c^{\dagger}_{\vec{k},\sigma}c_{\vec{k},\sigma} + 4V\langle T_z\rangle i\sum_{\vec{k},\sigma}\tilde{\gamma}_k c^{\dagger}_{\vec{k}+\vec{Q},\sigma}c_{\vec{k},\sigma}$$
$$+4V\sum_{\vec{k}}\tilde{\gamma}_k(\Delta c^{\dagger}_{\vec{k},\uparrow}c^{\dagger}_{-\vec{k},\downarrow} + \Delta^* c_{-\vec{k},\downarrow}c_{\vec{k},\uparrow}) + 4NV(|\Delta|^2+\langle O_n\rangle^2+\langle T_x\rangle^2+\langle T\rangle^2), \tag{16}$$

where $\langle T\rangle^2=\langle T_x\rangle^2+\langle T_y\rangle^2+\langle T_z\rangle^2$ and $\tilde{\gamma}_k=(c_x-c_y)/2$. The first two terms in Eq. (16) renormalize the chemical potential and the hopping t, respectively, and can be neglected. The terms in $\langle T_i\rangle$ comprise a pseudospin triplet of CDW-like distortions, with T_x representing a CDW similar to the one discussed above, T_y being related to the low-temperature tetragonal distortion and T_z an orbital antiferromagnet closely related to the flux phase. The remaining term is a *d*-wave superconductor. The coefficients of the terms must be found self-consistently by solving the gap equations

$$\sum_{\sigma}\langle c^{\dagger}_{i,\sigma}c_{i,\sigma}\rangle = 1-x+2(-1)^{\vec{r}_i}\langle T_x\rangle, \tag{17}$$

$$\mathrm{Im}\langle c^{\dagger}_{i,\sigma}c_{i+\hat{x},\sigma}\rangle = -\mathrm{Im}\langle c^{\dagger}_{i,\sigma}c_{i+\hat{y},\sigma}\rangle = (-1)^{\vec{r}_i}\langle T_z\rangle, \tag{18}$$

$$\mathrm{Re}\langle c^{\dagger}_{i,\sigma}c_{i+\hat{x},\sigma}\rangle = \langle O_n\rangle+\langle T_y\rangle,$$

$$\mathrm{Re}\langle c^{\dagger}_{i,\sigma}c_{i+\hat{y},\sigma}\rangle = \langle O_n\rangle-\langle T_y\rangle, \tag{19}$$

$$\langle c^{\dagger}_{i\uparrow}c^{\dagger}_{i+\hat{x},\downarrow}\rangle = \Delta. \tag{20}$$

The terms $\langle O_n\rangle$ and $\langle T_y\rangle$ have recently been discussed by Valenzuela and Vozmediano.[33] A detailed discussion of the competition between the three CDW-like modes is given in Ref. 16.

3. d-wave superconductivity

Retaining only the superconducting term in Eq. (16), the interaction can be derived from a quartic term

$$H' = \sum_{\vec{k},\vec{l}} V_{\vec{k},\vec{l}}c^{\dagger}_{\vec{k},\uparrow}c^{\dagger}_{-\vec{k},\downarrow}c_{-\vec{l},\downarrow}c_{\vec{l},\uparrow}, \tag{21}$$

with $V_{\vec{k},\vec{l}}=2V[\cos(k_x-l_x)a+\cos(k_y-l_y)a]$. Assuming $\Delta_{\vec{k}}=\Delta_x\cos k_x a+\Delta_y\cos k_y a$, the gap equations can be written in the form

$$\Delta_i = \sum_{j=x,y} A_{i,j}\Delta_j \tag{22}$$

$(i=x,y)$, with

$$A_{i,j} = -2V\sum_{\vec{l}}\cos l_i a\cos l_j a\,\frac{\tanh E_{\vec{l}}/2k_BT}{2E_{\vec{l}}} \tag{23}$$

and $E_{\vec{l}}=\sqrt{(\epsilon_{\vec{l}}-e_F)^2+\Delta^2_{\vec{l}}}$.

For the uniform charged state (infinitely wide stripe) $A_{x,x}=A_{y,y}$, and the gap symmetry can be simply analyzed. The symmetry can be either *d* wave ($\Delta_y=-\Delta_x$) or extended *s* wave ($\Delta_y=+\Delta_x$), with the choice $A_{x,y}\Delta_x\Delta_y>0$ giving the largest gap. The $A_{x,x}$ term is always BCS like, having the opposite sign from V, while the $A_{x,y}$ term has the opposite sign from $A_{x,x}$, the integral being dominated by the regions near the VHS's. Hence, there are two possibilities: (i) attractive ($V<0$) *d*-wave superconductivity or (ii) repulsive ($V>0$) extended *s*-wave superconductivity. However, the latter would require $|A_{x,y}|>|A_{x,x}|$, which does not arise in the present model, so only case (i) is possible. These considerations readily generalize to a finite-width stripe, for which $A_{x,x}\neq A_{y,y}$.

Agterberg *et al.*[34] recently introduced a model for "exotic" superconductivity in multiband superconductors. If the Fermi surface consists of several inequivalent but degenerate pockets, the order parameter can consist of symmetry-allowed superpositions of the order parameters of the individual pockets. Equation (23) can be thought of as a form of exotic superconductivity, with the degenerate VHS's playing the role of hole pockets.

B. Modifications due to magnetic order

In the above calculations, it was implicitly assumed that the doping is high enough that the only role of the on-site

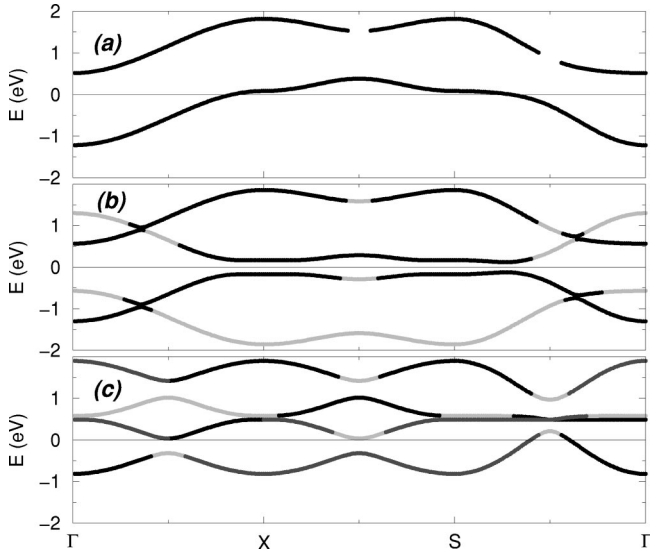

FIG. 6. Dispersion of linear antiferromagnetic (LAF) array along the linear direction (X) (a), along with modifications due to d-wave superconductivity (b) or CDW order (c). $U/t=6, t'/t=0$, $V/t=2$ (b), 0.1 (c).

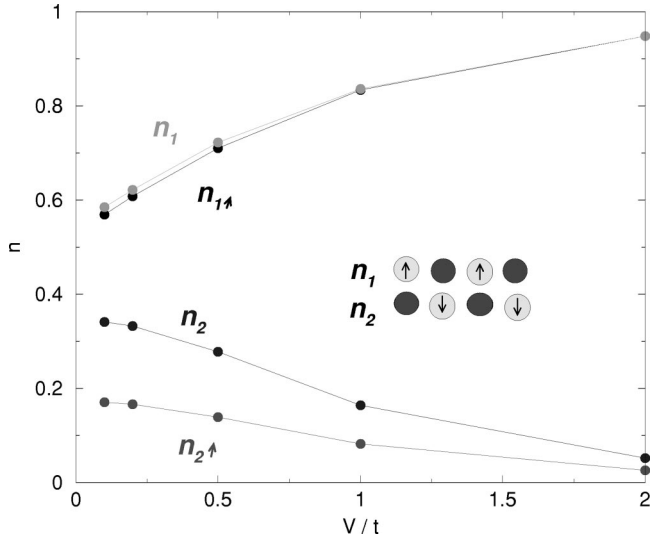

FIG. 7. Linear antiferromagnetic (LAF) array with CDW's, showing spin and doping distribution on different sites as a function of interaction strength V, with $U/t=6, t'/t=-0.276$. The inset shows the arrangement of atoms.

repulsion U is to renormalize the band parameters. However, Baskaran[35] recently estimated that near-optimal doping correlation effects remain stronger than the kinetic energy associated with hopping. Hence, it is important to look for stripe ground states which minimize this on-site repulsion (class B stripes). The LAF stripes discussed in Sec. III are a good candidate for the cuprate charged stripes: they closely resemble the White-Scalapino stripes,[13] have an appropriate doping, close to $x_0=0.25$, include strong correlations, and have the additional advantage that a two-cell-wide LAF charge stripe acts as a natural APB for the AF stripes. In this section, we will explore these stripes and show that they can be further stabilized by additional interactions.

A special form of strongly correlated CDW is found to exist on a LAF. The charge and spin distribution is shown in the inset to Fig. 7, with the corresponding dispersion in Fig. 6(c). There is a strong antiferromagnetic ordering on one sublattice, while most of the holes are confined on the other, nonmagnetic sublattice. Whereas in a conventional CDW the charge density is zero on one sublattice and two on the other, in this strong-coupling case the hole density varies from 0 to 1, and there is no double occupancy, Fig. 7. Whereas the paramagnetic stripes were extremely sensitive to quantum confinement, these magnetic charged stripes are much less so: this CDW is stable almost independently of the stripe width. From Fig. 6(c), it can be seen that the gapped Fermi surface still has hole pockets near $(\pi/2,\pi/2)$, which would lead to conducting stripes, consistent with optical properties.[36] However, it is only found near a hole doping $x=0.5$, and so does not appear to be relevant for stripe physics in the cuprates.

Away from this doping, CDW instabilities are relatively weak and it is possible to stabilize d-wave superconductivity, Figs. 6(b) and 8. While the overall dispersion varies with stripe width the superconducting gap is also relatively insensitive to the width and actually increases for the narrowest stripes, Fig. 9. Note that the order parameter is not a pure d wave, the gap along the stripe being larger. Such a large anisotropy is not consistent with tunneling measurements of the gap; it is possible that the anisotropy is reduced by strong interstripe coupling. On the other hand, a large gap anisotropy has been found in YBCO,[37] where the stripes are aligned along the chain direction.[3]

Note in Figs. 6(b) and 8 that the combination of LAF and d-wave order leads to a finite minimum gap over the full Fermi surface. While the pure LAF phase is not stabilized by the VHS, the d-wave superconductivity is optimized when the Fermi level is at the $(\pi,0)$ VHS—at essentially the *same doping*, $x_0=0.245$, as the VHS on a paramagnetic stripe.

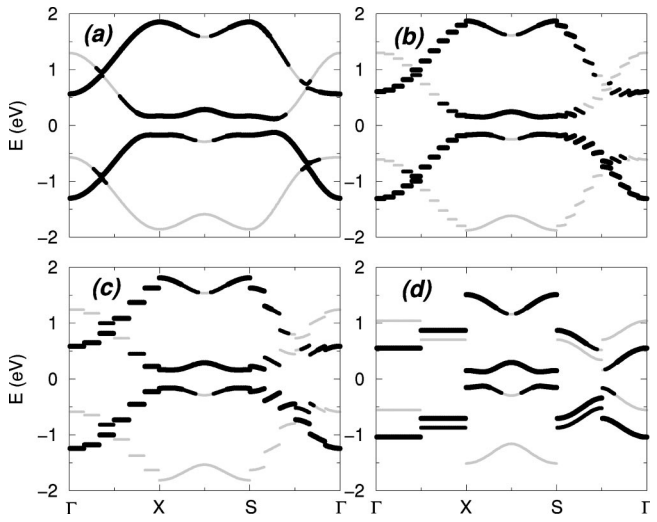

FIG. 8. Dispersion of a LAF with d-wave superconducting order for a uniform system (a) or a single stripe of width $N=10$ (b), 6 (c), or 2 (d) atoms. Darkness of lines reflects the relative intensity of the dispersion feature.

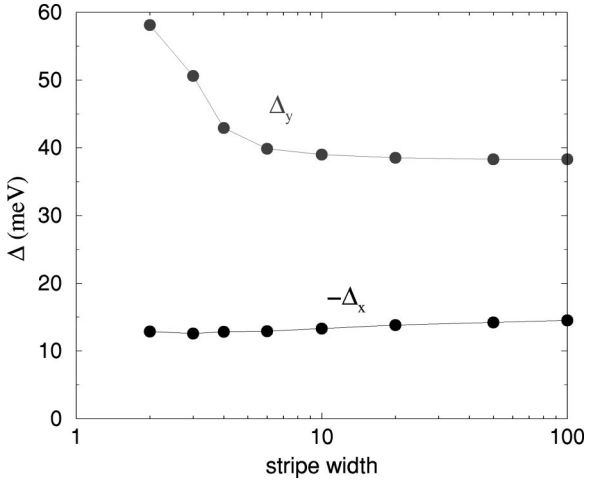

FIG. 9. Linear antiferromagnetic (LAF) array with "*d*-wave" superconductivity, showing the magnitude of the gap along (*y*) or across (*x*) the stripes, as a function of stripe width.

VI. EXTENSION TO ARRAYS

In Ref. 9, the Fermi surface was calculated for a series of ordered stripe arrays. These results can now be compared to experimental photoemission data.[38] For this purpose we replot the data as integrated spectral weight over a finite energy cut within energy ΔE of the Fermi surface. Figure 10(a) shows a cut with $\Delta E = 200$ meV for the model of a 1/8 doped stripe array (i.e., $x = 0.125$).[9] The pattern is readily understood: the stripe superlattice leads to a number of quasi-one-dimensional bands; however, due to structure factor effects, they have significant intensity only near the original Fermi surface [solid line in Fig. 10(a)]. For comparison with experiment, the calculated spectral weight is symmetrized $(0,\pi) \leftrightarrow (\pi,0)$ in Fig. 10(b) to represent a sample with regions of stripes running along both *X* and *Y* directions. Finally, an empirical matrix element is included, Fig. 10(c), which extinguishes spectral weight along the zone diagonal, $(0,0) \rightarrow (\pi,\pi)$, similar to the matrix element assumed in analyzing Bi2212.[38,39] The resulting Fermi surface maps for several values of ΔE are illustrated in Ref. 12 for paramagnetic charged stripes, and in Figs. 11 ($x = 1/8$) and 12 ($x = 0.1875$) for LAF stripes.

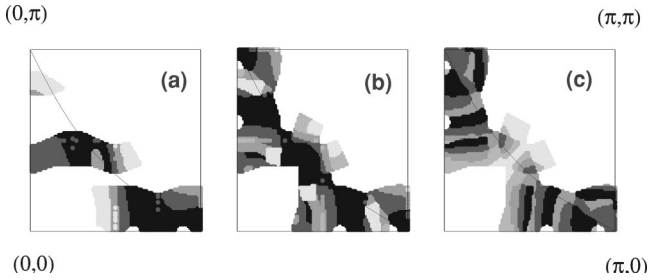

FIG. 10. Constant-energy cuts of photoemission dispersion for a (2,2) stripe array, within 200 meV of the Fermi level. Lines = Fermi surface of bulk (or very wide) charged stripes. Relative intensity increases with darker shading. (a) Representative of a single domain sample; (b) for a multidomain sample (symmetrized about the zone diagonal); (c) with a diagonal-suppressing matrix element, $M = |c_x - c_y|$.

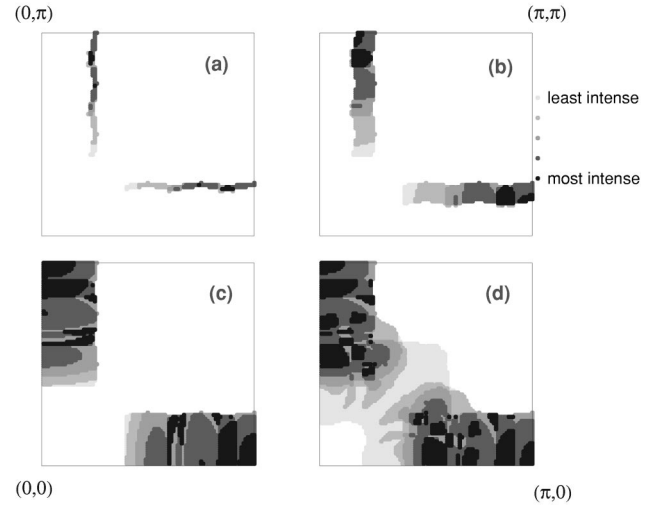

FIG. 11. Constant-energy cuts of photoemission dispersion for a (2,2) stripe array, with LAF charged stripes, within (a) 30, (b) 100, (c) 200, or (d) 500 meV of the Fermi level.

For both models, the stripe band nearest $(\pi,0)$ is in good agreement with experiment: there is little dispersion perpendicular to the stripe, while the intensity falls off toward (0,0) due to the structure factor effect. In general, the LAF stripes are in better agreement with experiment, since the additional subbands predicted for paramagnetic stripes [moving from $(\pi,0)$ toward $(0,\pi)$] are not seen in the experiment. While the matrix element improves the agreement, theory suggests that this effect is present only for certain photon polarizations.[40] One disagreement with experiment for both models is that for shallow energy cuts (30, 100 meV) the experiment still finds a smeared dispersion rather than a

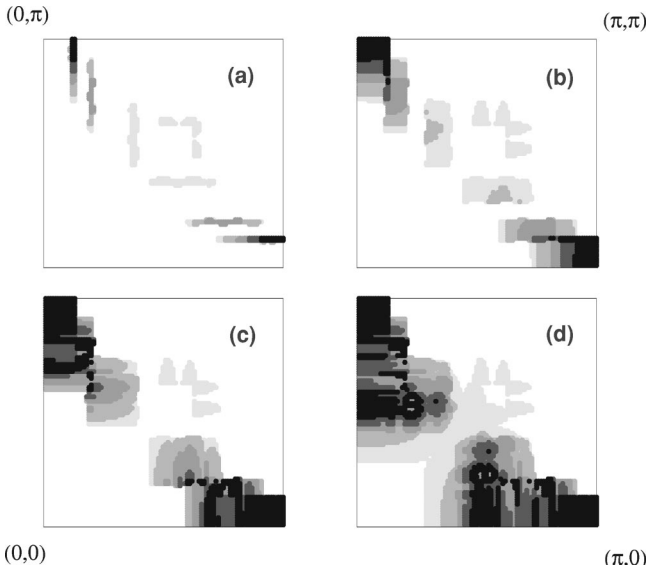

FIG. 12. Constant-energy cuts of photoemission dispersion for a (2,6) stripe array, with LAF charged stripes, within (a) 30, (b) 100, (c) 200, or (d) 500 meV of the Fermi level.

sharp Fermi surface. This is presumably an effect of stripe fluctuations.

It should be noted that all the spectral weight in Figs. 10–12 is associated with the charged stripes; the lower Hubbard band of the AFM stripes lies below 0.5 eV in LSCO. It is somewhat surprising that the spectral weight nearest the Fermi level is near $(\pi,0)$, since this is where the pseudogap arises. Nevertheless, our calculation reproduces both the (quantum confinement) pseudogap, Fig. 4, and the spectral weight distribution.

VII. DISCUSSION

A. Evidence for charge stripe doping $x_0=0.25$

1. Doping on charged stripes

Recent evidence suggests that the stripes and pseudogap terminate at the same doping x_0 while superconductivity persists to higher doping.[6] However, the proper choice of x_0 requires some discussion. The neutron diffraction measurements of Tranquada *et al.*[2] and Yamada *et al.*[1] have established that charged stripes in $La_{2-x}Sr_xCuO_4$ (LSCO) have an invariant topology over the doping range $0.06\leqslant x\leqslant 0.125$, acting as APB's for the AFM stripes and having a net doping of 0.5 holes per stripe. However, there are two models for how this charge is distributed: either in one row with average hole density 0.5 hole per copper site or in two rows with 0.25 hole per copper. These two alternatives are often somewhat simplistically referred to as site order versus bond order. The strongest evidence distinguishing between the alternatives comes from x-ray data on the charge order[41] at $x=1/8$: nonobservation of diffraction harmonics suggests a sinusoidal distribution of charge. For a four-Cu-wide repeat distance, two insulating and two charged rows would be exactly sinusoidal, whereas one charged and three insulating rows should have significant harmonic content. A similar conclusion was reached by muon spin resonance (μSR) line shape analysis.[42] However, the charge ordering peaks are weak, and it remains possible that fluctuations or disorder could wash out the harmonics.

Direct evidence for the density on the charged stripes is found from low-temperature nuclear quadrupole resonance (NQR) measurements,[43] which find values $x_0\sim 0.18$–0.19. While this is close to the lower value, the small difference can also be understood: this is a *local* measurement, and it is expected that some holes will be pushed off onto the magnetic stripes. The lower doping is also more consistent with the *t-j* model simulations of White and Scalapino.[13] Indirect evidence favoring the lower hole density includes the fact that it is easier to understand the properties of AFM stripes in terms of even-leg ladders (e.g., the AFM stripes would be two coppers wide at $x=1/8$),[44] and that the stripe phase appears to terminate when the average doping approaches $x=0.25$, as discussed below.

2. Doping at termination of the stripe phase

We assume that the pseudogap is associated with an order parameter which competes with superconductivity, representing either magnetic[45,46] or charge-density-wave[19,47] order, but in either case associated with stripes.[48,9,49] Similarly, a pseudogap arises in the nickelates[50] in conjunction with stripe fluctuations and turns into a true gap at the charge ordering temperature. Therefore, the fact that the pseudogap closes in the overdoped regime in the cuprates strongly suggests that stripes terminate at the same doping, as a form of quantum critical point (QCP).[51,8] In an EPS model, this doping should also be x_0, and we present evidence that this is the case.

Tallon[52] finds an optimal doping at $x_{opt}=0.16$ for all cuprates, with respect to which the stripes terminate at a doping $x=0.19$. However, it is hard to reconcile a common optimal doping with muon spin resonance data,[53] which find T_c is optimized at very different values of n_s/m (n_s is the pair density, which seems to scale with the hole doping,[54] and m effective mass) for LSCO and YBCO. We assume instead that m is approximately constant, so x_{opt} scales with n/m; thus, if $x_{opt}=0.16$ for LSCO, it is 0.21 for YBCO, in good agreement with several estimates.[55] This also resolves a problem with the thermopower. While the thermopower appears to be universal for most cuprates and the best means of estimating the doping is from room-temperature thermopower, LSCO is anomalous in that ''overdoped'' samples still have high thermopower.[56] If the doping for YBCO is rescaled as above, however, the thermopower data of LSCO fall on the universal curve. Hence, the anomaly for LSCO is not in the thermopower, but in a too low value of T_c, which is accompanied by a too low value of x_{opt}. It is likely that these features are associated with a competing LTT phase, which is most prominent in LSCO and which also leads to the most nearly static stripe correlations.

Taking $x_{opt}=0.21$ for YBCO gives $x_0=19/16\times 0.21=0.25$, which agrees with the above estimate for the doping on the charged stripes, x_0. We believe this value holds for *all cuprates*, including LSCO, as shown below. This would lead to very wide charged stripes near optimal doping: the width of the charged stripes, N, satisfies $N/(N+2)=16/19$ or $N=32/3\simeq 10$ Cu wide. Hence, models of isolated quasi-one-dimensional charged stripes are likely to be valid only in the far-underdoped regime, while for the good superconductors a better model would be a metal with intrinsic weak links.[57]

Here we show that strong magnetic correlations extrapolate to zero (i.e., magnetic stripes disappear) at the same doping for which the pseudogap closes.[9,6,58,3] Figure 13(a) compares the intensity I of the integrated inelastic neutron scattering near (π,π) as a function of doping in YBCO (Ref. 59) and LSCO.[2,1] In a stripe picture, I should be a measure of the fraction of material in AFM stripes. Remarkably, the intensity extrapolates to zero at nearly the same doping in both materials, even though $T_c(x)$ peaks at substantially different dopings. For both materials, this is the doping at which the pseudogap closes. Furthermore, a study of the neutron diffraction pair distribution function[60] for LSCO finds evidence for charge fluctuations, presumably associated with stripes. The excess fluctuations are maximal near $x=0.15$ and terminate near $x=0.25$. Strong reductions of thermal conductivity associated with stripe scattering also terminate at a compa-

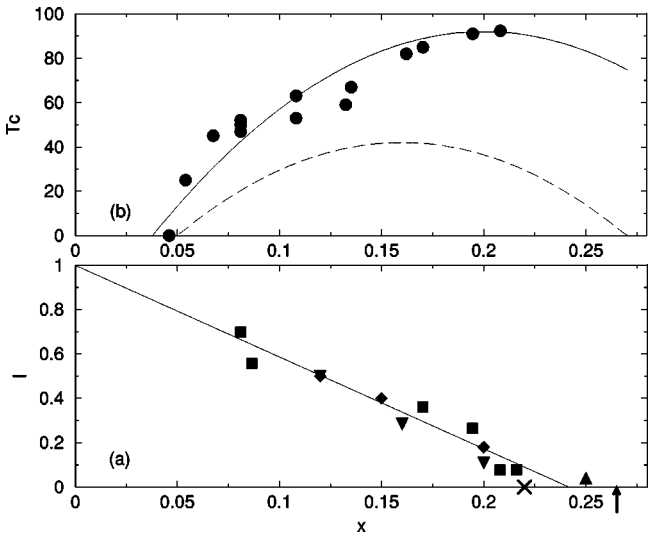

FIG. 13. (a) Magnetic inelastic scattering intensity vs x in YBCO [squares (Ref. 59)] and LSCO [diamonds (Ref. 2) and triangle (Ref. 1)]. Inverted triangles = (scaled) effective exchange constant in RE-substituted LSCO, estimated from slowing of spin fluctuations (Ref. 64). (b) Corresponding $T_c(x)$: solid line = YBCO [circles (Ref. 59)]; dashed line = LSCO.

rable doping,[61] while a recent optical study[62] finds evidence for a quantum critical point at a similar doping, $x\sim 0.22$. Moreover, in Bi2212, Tokunaga *et al.*[63] have introduced a new crossover temperature T_{mK} based on Cu NMR, below which AFM correlations develop; they find $T_{mK}\rightarrow 0$ near $x=0.26$.

A recent NQR study of the slowing of spin fluctuations in rare-earth (RE-) substituted LSCO (Ref. 64) finds that the effective spin stiffness ρ_s^{eff} (or equivalently the effective exchange constant) scales to zero at a comparable doping; the inverted triangles in Fig. 13 show $2\pi\rho_s^{eff}/460$ K. There is a 1/8 anomaly, in that the doping dependence of ρ_s^{eff} changes radically below $x=0.12$. Note that while the integrated neutron intensity scales approximately with the area fraction of charged stripes, $2\pi\rho_s^{eff}$ scales to ~ 460 K as $x\rightarrow 0$. This is only 1/4 of the actual spin stiffness, $2\pi\rho_s=1.13J=1730$ K in the undoped AFM. The change by nearly a factor of 4 is suggestive of a dimensional reduction (lower coordination), but for an isolated straight spin ladder, a factor of 2 might have been expected.

It is important to note the proximity of this termination of the phase separation regime to the VHS: the arrow in Fig. 13(a) shows the doping at which the pseudogap in the heat capacity[65] closes, leaving an approximately logarithmic peak,[24] while the $\times$ indicates the point at which photoemission finds the VHS crossing the Fermi level.[66] Termination of the stripe phase close to a VHS is an important prediction of our EPS model of stripes.

Figure 13 provides strong constraints on the value of x_0. LSCO is the only cuprate for which the value of x is measured directly, and a value $x_0=0.19$ for the stripe termination is clearly too low for LSCO: when the stripes are gone, magnetic correlations should be weak, but there is evidence for long-range magnetic order at $x=0.2$[2] and 0.21, the latter coupled with a suppression of T_c.[67] On the other hand, both facts are compatible with $x_0\sim 0.25$, Fig. 13.

3. Crossover at 1/8 doping

For $x_0\sim 1/4$, the crossover $x_{cr}=x_0/2$ can be identified with the 1/8 anomaly, where both charged and AFM stripes have their minimal width (two Cu atoms). There is considerable evidence that the doping 1/8, in addition to its special stability, acts as a crossover in the properties of the stripes. Thus, Uchida *et al.*,[68] studying the Hall coefficient R_H, find a crossover from one-dimensional behavior ($R_H\rightarrow 0$ as $T\rightarrow 0$) for $x<x_{cr}=1/8$ to two-dimensional behavior (coupled charged stripes) for $x>x_{cr}$. In YBCO, the spin gap grows slowly with doping for $x<x_{cr}$, then more rapidly for $x>x_{cr}$; this behavior can be understood in terms of coupled spin ladders, as the coupling changes with the width of the charged stripes.[9] In Eu-substituted LSCO,[69] the Meissner fraction is negligibly small for $x<x_{cr}$, then grows roughly linearly with doping until $x\simeq 0.18$, staying large up to at least $x=0.22$. Finally, the two-magnon Raman peak in LSCO has a splitting at low temperatures which has been associated with stripes,[70] in analogy with similar observations in $La_{2-x}Sr_xNiO_4$ (LSNO).[71] For $x<x_{cr}$ the ratio of the two peak frequencies is constant and consistent with a simple stripe model; for $x>x_{cr}$ the lower frequency starts decreasing with doping. Moreover, the higher frequency loses intensity with doping; near $x=0.26$, the *intensity* of one mode approximately disappears, while the *frequency* of the other mode extrapolates to zero.

4. Clusters for x>1/8

The Yamada[1,2,72] plot, Fig. 14(a), provides a severe constraint on any model of stripes: in LSCO the incommensurability δ is found to grow linearly with doping for $x<x_{cr}$ but to saturate for $x>x_{cr}$. Furthermore, the saturation value is just the incommensurability expected for $x=1/8$ doped stripes, $\delta_{sat}=x_{cr}$. A similar saturation has been reported in YBCO, but different groups find different values for δ_{sat}: $\sim 1/6$ (Ref. 73) or $\sim 1/10$ (Ref. 74). If either of these values proves correct, it would suggest some nonuniversality in x_0, perhaps associated with bilayer splitting.

For $x\leqslant 1/8$, the EPS model agrees with the Yamada plot, Fig. 14(b): an increase in doping causes the AFM stripes to narrow, with no changes in the charged stripes. Note that, for concreteness, we have assumed that the charged stripes have LAF order (Sec. III); these stripes naturally act as APB's, consistent with the neutron evidence. However, a simple extension of the stripe model for $x>1/8$ is in disagreement with the Yamada plot, Fig. 14(c): as the charge stripes get wider, and the incommensurability should decrease, while the neutron peaks may broaden if the wider charge stripes do not act as APB's. This behavior is not observed. However, the model can be simply modified to explain the observed saturation, Figs. 14(d) and 14(e). This would be a commensurability effect, with part of the sample pinned at 1/8 doping while the rest forms a different phase (e.g., at 1/4 doping) where no stripes are present. Such behavior is well known in nick-

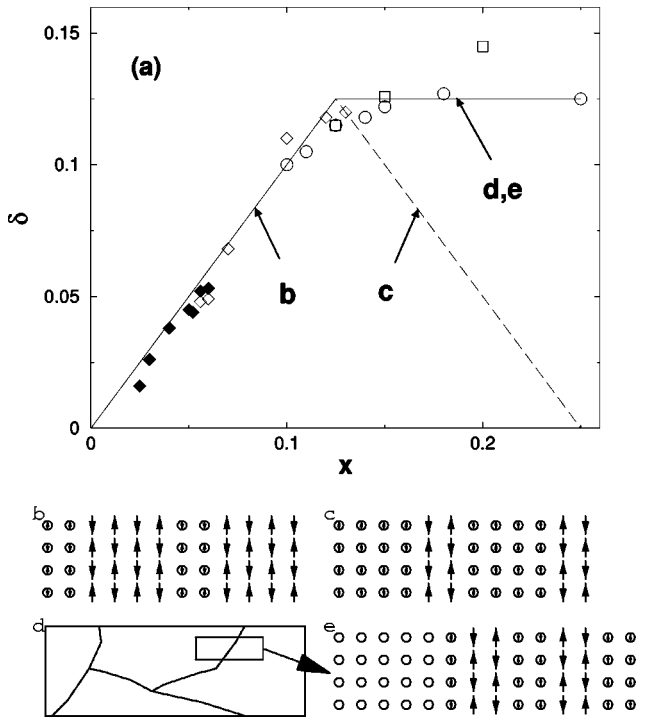

FIG. 14. (a) Yamada plot of incommensurability δ vs doping x for LSCO. Open squares = elastic neutron scattering in Nd-substituted samples (Ref. 2); others = inelastic neutron scattering for vertical stripes [open circles (Ref. 1) or diamonds (Ref. 72)] or diagonal stripes [solid diamonds (Ref. 72)]. Dashed (solid) line = prediction of EPS model without (with) commensurability effect at 1/8 doping. (b),(c) = Stripe phase model without commensurability effect, at $x=1/12$ (b) and 1/6 (c). For this figure, the charged stripes are assumed to have linear antiferromagnetic order (Sec. III). (d),(e) = domains associated with commensurability pinning of 1/8 doped phase; (e) = blowup of (d).

elates, where the coexistence of 1/3 and 1/2 stripes is common.

Further evidence for commensurability pinning is found by noting[12] the similar doping dependence of the chemical potential μ in LSCO (Ref. 75) and LSNO (Ref. 76), where the latter is clearly caused by commensurability pinning of a striped phase. The recent STM observations of local charged domains in Bi2212 (Ref. 4) paint a similar picture. The observed broad gap distribution is presumably due to the sensitivity of the EPS to the local density of charged impurities, presumably interstitial oxygen in Bi2212. This sensitivity to impurities leads to the question of which came first: is a preexisting EPS sensitive to local impurities, or does oxygen clustering[77] provide the driving mechanism for domain formation? Since the electronic inhomogeneity seems characteristic of most cuprates while there is considerable variety in the doping counterions, the simpler interpretation would appear to be that the EPS is primary. Thus, in $La_2CuO_{4+\delta}$ (LCO), the interstitial oxygens are highly mobile, allowing the domains to grow to macroscopic size. Similar clusters form in YBCO (here associated with chain oxygens), but can be suppressed in fully oxygenated samples by quenching.[78] On the other hand, well-formed stripes appear when the doping counterions are least mobile in LSCO. Microwave anomalies in Bi2212 have been interpreted in terms of similar electronic domains,[5] suggesting that they are representative of the bulk, while measurements on other cuprates[79] find similar anomalous behavior which was interpreted in terms of pinned CDW's, possibly stripe related. A domain picture would also explain the persistence of nodal quasiparticles in the underdoped regime, at least down to 1/8 doping.[80]

In conclusion, the assumption of a charged stripe doping $x_0 \simeq 0.25$ reconciles the neutron diffraction data, evidence for a termination of the stripe phase near x_0, and the 1/8 anomaly as a crossover effect near $x_0/2$, while commensurability effects can explain the saturation in the Yamada plot and the STM observation of charge domains.

B. Superconductivity in charged stripes

We suggested earlier[9] that the peak and hump features seen in photoemission from Bi2212 were associated with the charged and the AFM stripes, respectively. As such, the intensity of the peak should have the doping dependence predicted for charged stripes, with the intensity increasing from zero at half filling, approximately linearly with doping x. This has now been verified experimentally.[66,81] Moreover, the maximum intensity of the spectral weight occurs at the same doping[66] x_0 discussed above, where the stripe phase terminates. Remarkably, the peak spectral weight closely tracks T_c, suggesting that the *superconducting pairs "live" in the charged stripes*, as predicted by several models.[24,82] Consistent with this, a number of measures of the strength of superconductivity (condensation energy, critical current) are optimized at this same point[66,6,83] where the charge stripe intensity is maximum and AFM stripes vanish. The fact that T_c itself is actually optimized at a slightly lower doping may be a hint that stripes can enhance the superconducting gap, as found above, Fig. 9. An analysis of the superconducting fluctuations in the underdoped cuprates[84] leads to similar conclusions: superconductivity arises predominantly in the charged stripes (or domains), so the phase coherence temperature falls in underdoped cuprates, due to weak coupling between domains. Remarkably, the mean-field transition temperature is enhanced in the underdoped regime, consistent with the theoretical results of Fig. 9.

VIII. CONCLUSIONS

Recent experiments have provided considerable evidence for the presence of stripes and EPS in the cuprates, but there remain many questions as to how universal these are, how they arise and vary with doping, and how they interact with superconductivity. We have here elaborated our earlier[9] model of stripes driven by frustrated phase separation, in particular adducing evidence that the doping on the charged stripes is close to $x=x_0=0.25$ and that when the average doping approaches this value EPS terminates. Moreover, near $x_{cr}=x_0/2$ there is a crossover in stripe properties: for $x<x_{cr}$ the charged stripes are quantum confined, and for $x>x_{cr}$ the AFM stripes are so confined. This model can explain the 1/8 anomaly ($x=x_{cr}$), the anomalous Hall effect ($R_H \to 0$) (Ref. 68) for $x<1/8$ (charged stripes confined,

hence one dimensional), and the growing spin gap in YBCO for $x>1/8$.[9]

On the important issue of the *structure* of a charged stripe, we have explored a number of possibilities without coming to any final conclusions. While there is evidence that superconductivity ''lives'' in the charged stripes, there also appears to be a second instability in these stripes, which stabilizes the stripe phase while competing with superconductivity. We have shown that a semiquantitative understanding can be achieved by looking at the properties of a single doped ladder, and we have discussed how a number of instabilities (both CDW and superconducting) vary with ladder width. We showed that strong correlation effects could lead to charged stripes with a residual magnetic order, introduced a simple model for White-Scalapino-like stripes, and found novel superconducting and CDW instabilities associated with such stripes. We illustrated how stripe order would affect angle-resolved photoemission spectroscopy (ARPES) spectra, both dispersions and Fermi surface maps. Future studies will apply the model to describing other properties of the cuprates.

Certain anomalous features of strong-correlation calculations may find an explanation in underlying phase separation. Thus, the vanishing of the renormalized hopping parameter t near half filling in slave boson calculations may reflect the vanishing of the charged stripes at half filling,[9] while the frequently observed pinning of the VHS near the Fermi level[24,85] is consistent with VHS-stabilized charged stripes.

Finally, the idea of a commensurability effect near 1/8 doping, leading to a coexistence of *domains* for $x>1/8$, provides a simple explanation for a large variety of experimental findings, including the saturation of the Yamada plot, the direct observation of domains in STM studies, and a variety of microwave anomalies. This may also lead to a resolution of the combined puzzle of magnetic neutron scattering incommensurability and the neutron resonance peak. A stripe model provides a natural explanation of the incommensurability for $x\leqslant 1/8$, including a stripe reorientation transition at the metal-superconductor transition near $x\sim 0.053$. However, a band picture[86] (with E_F close to a VHS) provides a superior model for the combined, frequency-dependent incommensurability *cum* resonance peak found near-optimal doping in YBCO and Bi2212. An EPS crossover from stripes to domains near $x\sim 1/8$ would provide a natural explanation of these phenomena.

ACKNOWLEDGMENTS

These computations were carried out using the facilities of the Advanced Scientific Computation Center at Northeastern University (NU-ASCC). Their support is gratefully acknowledged. We had stimulating conversations with S. Pan and J.C. Davis. C.K.'s research was supported in part by NSF Grant No. NSF-9711910.

[1] K. Yamada, C. H. Lee, K. Kurahashi, J. Wada, S. Wakimoto, S. Ueki, H. Kimura, Y. Endoh, S. Hosoya, G. Shirane, R. J. Birgeneau, M. Greven, M. A. Kastner, and Y. J. Kim, Phys. Rev. B **57**, 6165 (1998).

[2] J. M. Tranquada, B. J. Sternlieb, J. D. Axe, Y. Nakamura, and S. Uchida, Nature (London) **375**, 561 (1995); J. M. Tranquada, J. D. Axe, N. Ichikawa, A. R. Moodenbaugh, Y. Nakamura, and S. Uchida, Phys. Rev. Lett. **78**, 338 (1997).

[3] H. A. Mook (unpublished); H. A. Mook and F. Doğan, Nature (London) **401**, 145 (1999); Physica C **364-5**, 553 (2001).

[4] T. Cren, D. Roditchev, W. Sacks, J. Klein, J.-B. Moussy, C. Deville-Cavellin, and M. Laguës, Phys. Rev. Lett. **84**, 147 (2000); C. Howald, P. Fournier, and A. Kapitulnik, Phys. Rev. B **64**, 100504 (2001); S. H. Pan, J. P. O'Neal, R. L. Badzey, C. Chamon, H. Ding, J. R. Engelbrecht, Z. Wang, H. Eisaki, S. Uchida, A. K. Gupta, K.-W. Ng, E. W. Hudson, K. M. Lang, and J. C. Davis, Nature (London) **413**, 282 (2001); J. C. Davis (unpublished).

[5] J. Orenstein (unpublished).

[6] J. L. Tallon, cond-mat/9911422 (unpublished); J. L. Tallon, J. W. Loram, and G. V. M. Williams, cond-mat/991423 (unpublished); J. L. Tallon, J. W. Loram, G. V. M. Williams, J. R. Cooper, I. R. Fisher, J. D. Johnson, M. P. Staines, and C. Bernhard, Phys. Status Solidi B **215**, 531 (1999).

[7] M. I. Salkola, V. J. Emery, and S. A. Kivelson, Phys. Rev. Lett. **77**, 155 (1996).

[8] S. Caprara, C. Di Castro, M. Grilli, A. Perali, and M. Sulpizi, Physica C **317-8**, 230 (1999); G. Seibold, F. Becca, F. Bucci, C. Castellani, C. di Castro, and M. Grilli, cond-mat/9906108 (unpublished).

[9] R. S. Markiewicz, Phys. Rev. B **62**, 1252 (2000).

[10] M. G. Zacher, R. Eder, E. Arrigoni, and W. Hanke, Phys. Rev. Lett. **85**, 2585 (2000).

[11] J. Eroles, G. Ortiz, A. V. Balatsky, and A. R. Bishop, Phys. Rev. B **64**, 174510 (2001).

[12] R. S. Markiewicz and C. Kusko, Int. J. Mod. Phys. B **14**, 3561 (2000).

[13] S. R. White and D. J. Scalapino, Phys. Rev. Lett. **80**, 1272 (1998); **81**, 3227 (1998).

[14] J. Hafner, *From Hamiltonians to Phase Diagrams* (Springer, Berlin, 1987).

[15] P. W. Anderson (unpublished); *The Theory of High-T_c Superconductivity* (Princeton University Press, Princeton, 1997).

[16] R. S. Markiewicz and C. Kusko, cond-mat/0102452 (unpublished).

[17] Y.-S. Yi, Z.-G. Yu, A. R. Bishop, and J. T. Gammel, Phys. Rev. B **58**, 503 (1998).

[18] T. Tohyama, S. Nagai, Y. Shibata, and S. Maekawa, Phys. Rev. Lett. **82**, 4910 (1999).

[19] R. S. Markiewicz, Phys. Rev. B **56**, 9091 (1997).

[20] P. Fazekas, Found. Phys. **30**, 1999 (2000).

[21] C. Kusko and R. S. Markiewicz, cond-mat/0102440 (unpublished).

[22] R. Hlubina, S. Sorella, and F. Guinea, Phys. Rev. Lett. **78**, 1343 (1997); R. Hlubina, Phys. Rev. B **59**, 9600 (1999). See also D. Vollhardt, N. Blümer, K. Held, M. Kollar, J. Schlipf, and M.

Ulmke, Z. Phys. B: Condens. Matter **103**, 283 (1997).
[23] B. Valenzuela, M. Vozmediano, and F. Guinea, Phys. Rev. B **62**, 11 312 (2000); M. Vozmediano (personal communication).
[24] R. S. Markiewicz, J. Phys. Chem. Solids **58**, 1179 (1997).
[25] J. Fritzenkötter and K. Dichtel, in *Stripes and Related Phenomena*, edited by A. Bianconi and N. Saini (Kluwer Academic/Plenum, New York, 2000), p. 369.
[26] P. B. Visscher, Phys. Rev. B **10**, 943 (1974); E. L. Nagaev, *Physics of Magnetic Semiconductors* (Mir, Moscow, 1983).
[27] G. Su, Phys. Rev. B **54**, 8281 (1996); A. C. Cosentini, M. Capone, L. Guidoni, and G. B. Bachelet, *ibid.* **58**, 14 685 (1998).
[28] W. O. Putikka, R. L. Glenister, and R. R. P. Singh, Phys. Rev. Lett. **73**, 170 (1994); C. T. Shih, Y. C. Chen, and T. K. Lee, Phys. Rev. B **57**, 627 (1998); M. Calandra, F. Becca, and S. Sorella, Phys. Rev. Lett. **81**, 5185 (1998).
[29] C. S. Hellberg and E. Manousakais, Phys. Rev. Lett. **78**, 4609 (1997); Phys. Rev. B **61**, 11 787 (2000).
[30] L. P. Pryadko, S. Kivelson, and D. W. Hone, Phys. Rev. Lett. **80**, 5651 (1998).
[31] R. S. Markiewicz, C. Kusko, and V. Kidambi, Phys. Rev. B **60**, 627 (1999).
[32] C. Balseiro and L. Falicov, Phys. Rev. B **20**, 4457 (1979).
[33] B. Valenzuela and M. A. H. Vozmediano, Phys. Rev. B **63**, 153103 (2000).
[34] D. F. Agterberg, V. Barzykin, and L. P. Gor'kov, Europhys. Lett. **48**, 449 (1999); Phys. Rev. B **60**, 14 868 (2000).
[35] G. Baskaran, Phys. Rev. B **64**, 092506 (2001).
[36] R. S. Markiewicz (unpublished).
[37] D. H. Lu, D. L. Feng, N. P. Armitage, K. M. Shen, A. Damascelli, C. Kim, F. Ronning, Z.-X. Shen, D. A. Bonn, R. Liang, W. N. Hardy, A. I. Rykov, and S. Tajima, Phys. Rev. Lett. **86**, 4370 (2001).
[38] X. J. Zhou, P. Bogdanov, S. A. Kellar, T. Noda, H. Eisaki, S. Uchida, Z. Hussain, and Z.-X. Shen, Science **286**, 268 (1999).
[39] D. Orgad, S. A. Kivelson, E. W. Carlson, V. J. Emery, X. J. Zhou, and Z.-X. Shen, Phys. Rev. Lett. **86**, 4362 (2001).
[40] M. Lindroos and A. Bansil (personal communication).
[41] M. V. Zimmermann, A. Vigliante, T. Niemöller, N. Ichikawa, T. Frello, J. Madsen, P. Wochner, S. Uchida, N. H. Andersen, J. M. Tranquada, D. Gibbs, and J. R. Schneider, Europhys. Lett. **41**, 629 (1998); T. Niemoeller, N. Ichikawa, T. Frello, H. Huennefeld, N. H. Andersen, S. Uchida, J. R. Schneider, and J. M. Tranquada, cond-mat/9904383 (unpublished); T. Niemöller, H. Hünnefeld, T. Frello, N. H. Andersen, N. Ichikawa, S. Uchida, and J. R. Schneider, J. Low Temp. Phys. **117**, 455 (1999).
[42] K. M. Kojima, H. Eisaki, S. Uchida, Y. Fudamoto, I. M. Gat, A. Kinkhabwala, M. I. Larkin, G. M. Luke, and Y. J. Uemura, Physica B **289-90**, 343 (2000).
[43] G. B. Teitel'baum, B. Büchner, and H. de Gronkel, Phys. Rev. Lett. **84**, 2949 (2000).
[44] J. Tworzydlo, C. N. A. van Duin, and J. Zaanen, cond-mat/9808034, in Proceedings of the 2nd International Conference on Stripes and High Tc Superconductivity, Rome 1998, J. Supercond. (in press).
[45] A. Kampf and J. Schrieffer, Phys. Rev. B **41**, 6399 (1990).
[46] S.-C. Zhang, Science **275**, 1089 (1997).
[47] R. A. Klemm (unpublished); Physica C **341-8**, 839 (2000).
[48] C. Castellani, C. Di Castro, and M. Grilli, Phys. Rev. Lett. **75**, 4650 (1995).
[49] R. S. Markiewicz, Physica C **169**, 63 (1990).
[50] T. Katsufuji, T. Tanabe, T. Ishikawa, Y. Fukuda, T. Arima, and Y. Tokura, Phys. Rev. B **54**, 14 230 (1996).
[51] C. Sire, C. M. Varma, A. E. Ruckenstein, and T. Giamarchi, Phys. Rev. Lett. **72**, 2478 (1994).
[52] J. L. Tallon, Physica C **168**, 85 (1990).
[53] Y. J. Uemura, G. M. Luke, B. J. Sternlieb, J. H. Brewer, J. F. Carolan, W. N. Hardy, R. Kadano, J. R. Kempton, R. F. Kiefl, S. R. Kreitzman, P. Mulhern, T. M. Riseman, D. Ll. Williams, B. X. Yang, S. Uchida, H. Takagi, J. Gopalakrishnan, A. W. Sleight, M. A. Subramanian, C. L. Chien, M. Z. Cieplak, G. Xiao, V. Y. Lee, B. W. Statt, C. E. Stronach, W. J. Kossler, and X. H. Yu, Phys. Rev. Lett. **62**, 2317 (1989).
[54] Optical evidence that x and the superelectron density n_s both scale with T_c is found in H. L. Liu, M. A. Quijada, A. Zibold, Y.-D. Yoon, D. B. Tanner, G. Cao, J. E. Crow, H. Berger, G. Margaritondo, L. Forró, Beom-Hoan O, J. T. Markert, R. J. Kelly, and M. Onellion, J. Phys.: Condens. Matter **11**, 239 (1999).
[55] Consistent with $x_{opt}=0.21$ [Y. Tokura, J. B. Torrance, T. C. Huang, and A. I. Nazzal, Phys. Rev. B **38**, 7156 (1988)], 0.24 [U. Tutsch, P. Schweiss, R. Hauff, B. Obst, Th. Wolf, and H. Wühl, J. Low Temp. Phys. **117**, 951 (1999)], 0.2 [M. Merz, N. Nücker, P. Schweiss, S. Schuppler, C. T. Chen, V. Chakarian, J. Freeland, Y. U. Idzerta, M. Kläser, G. Müller-Vogt, and Th. Wolf, Phys. Rev. Lett. **80**, 5192 (1998)], and 0.21 [S. L. Drechsler, J. Malek, and H. Eschrig, Phys. Rev. B **55**, 606 (1997)]. A recent critique of Tallon's bond valence sum calculation (Ref. 52) also finds evidence for a larger x_{opt}, but concludes that the technique cannot accurately determine the mobile hole fraction on the CuO_2 planes [O. Chmaissem, Y. Eckstein, and C. G. Kuper, *ibid.* **63**, 174510 (2001)].
[56] J. L. Tallon, J. R. Cooper, P. S. I. P. N. de Silva, G. V. M. Williams, and J. W. Loram, Phys. Rev. Lett. **75**, 4114 (1995).
[57] E. C. Jones, D. C. Christen, J. R. Thompson, R. Feenstra, S. Zhu, D. H. Lowndes, J. M. Phillips, M. P. Siegal, and J. D. Budai, Phys. Rev. B **47**, 8986 (1993).
[58] P. Bourges, in *Neutron Scattering in Novel Materials*, edited by A. Furner (World Scientific, Singapore, 2000).
[59] P. Bourges, L. P. Regnault, J. Y Henry, C. Vettier, Y. Sidis, and P. Burlet, Physica B **215**, 30 (1995).
[60] E. S. Božin, G. H. Kwei, H. Takagi, and S. J. L. Billinge, Phys. Rev. Lett. **84**, 5856 (2000).
[61] O. Baberski, A. Lang, O. Maldonado, M. Hücker, B. Büchner, and A. Freimuth, Europhys. Lett. **44**, 335 (1998).
[62] T. Timusk, A. V. Puchkov, S. Doyle, A. M. Hermann, and N. N. Kolesnikov (unpublished).
[63] Y. Tokunaga, K. Ishida, K. Yoshida, T. Mito, Y. Kitaoka, Y. Nakayama, J. Shimoyama, K. Kishio, O. Narikiyo, and K. Miyake, Phys. Rev. B **284-88**, 663 (2000).
[64] A. W. Hunt, P. M. Singer, A. F. Cederström, and T. Imai, Phys. Rev. B **64**, 134525 (2001).
[65] J. W. Loram, J. L. Luo, J. R. Cooper, W. Y. Liang, and J. L. Tallon, Physica C **341-8**, 831 (2000).
[66] Z. X. Shen (unpublished); D. L. Feng, D. H. Lu, K. M. Shen, C. Kim, H. Eisaki, A. Damascelli, R. Yoshizaki, J.-i. Shimoyama, K. Kishio, G. Gu, S. Oh, A. Andrus, J. O'Donnell, J. N. Eckstein, and Z.-X. Shen, Science **280**, 277 (2000).
[67] Y. Koike, M. Akoshima, M. Aoyama, K. Nishimaki, T.

Kawamata, T. Adachi, T. Noji, I. Watanabe, S. Ohira, W. Higemoto, and K. Nagamine, Int. J. Mod. Phys. B **14**, 3520 (2000).
[68] T. Noda, H. Eisaki, and S. Uchida, Science **286**, 265 (1999).
[69] V. Kataev, B. Rameev, A. Validov, B. Büchner, M. Hücker, and R. Borowski, Phys. Rev. B **58**, 11 876 (1998).
[70] S. Sugai and N. Hayamizu, J. Phys. Chem. Solids **62**, 177 (2001).
[71] G. Blumberg, M. V. Klein, and S.-W. Cheong, Phys. Rev. Lett. **80**, 564 (1998); K. Yamamoto, T. Katsufuji, T. Tanabe, and Y. Tokura, *ibid.* **80**, 1493 (1998); and S. Sugai, N. Kitamori, S. Hosoya, and K. Yamada, J. Phys. Soc. Jpn. **67**, 2992 (1998).
[72] M. Fujita, K. Yamada, H. Hiraka, P. M. Gehring, S. H. Lee, S. Wakimoto, and G. Shirane, cond-mat/0101320 (unpublished).
[73] M. Arai, T. Nishijima, Y. Endoh, A. W. Garrett, S. Tajima, K. Tomimoto, Y. Shiohara, C. D. Frost, and S. M. Bennington, in *Cosmology and Particle Physics*, edited by R. Durrer *et al.*, AIP Conf.Proc. No. **554** (AIP, Melville, 2001), p. 191; M. Arai, Y. Endoh, S. Tajima, and S. M. Bennington, Int. J. Mod. Phys. B **14**, 3312 (2000).
[74] P. Dai, H. A. Mook, R. D. Hunt, and F. Dogan, Phys. Rev. B **63**, 054525 (2001).
[75] A. Ino, T. Mizokawa, A. Fujimori, K. Tamasaku, H. Eisaki, S. Uchida, T. Kimura, T. Sasagawa, and K. Kishio, Phys. Rev. Lett. **79**, 2101 (1997).
[76] M. Satake, K. Kobayashi, T. Mizokawa, A. Fujimori, T. Tanabe, T. Katsufuji, and Y. Tokura, Phys. Rev. B **61**, 15 515 (2000).
[77] A. V. Balatsky (unpublished). An oxygen clustering model has a problem, in that most of the excess oxygens in Bi-2212 are not randomly clustering, but are responsible for the superlattice formation. See W. Que and M. B. Walker, Phys. Rev. B **46**, 14 772 (1992).
[78] A. Erb, A. A. Manuel, M. Dhalle, F. Marti, J.-Y. Genoud, B. Revaz, A. Junod, D. Vasumathi, S. Ishibashi, A. Shukla, E. Walker, O. Fischer, R. Fluekiger, R. Pozzi, M. Mali, and D. Brinkmann, Solid State Commun. **112**, 245 (1999).
[79] C. Kusko, Z. Zhai, N. Hakim, R. S. Markiewicz, S. Sridhar, D. Colson, Viallet-Guillet, A. Forget, Yu. A. Nefyodov, M. R. Trunin, N. N. Kolesnikov, A. Maignan, A. Daignere, and A. Erb (unpublished); R. S. Markiewicz (unpublished).
[80] X. J. Zhou, T. Yoshida, S. A. Kellar, P. V. Bogdanov, E. D. Lu, A. Lanzara, M. Nakamura, T. Noda, T. Takeshita, H. Eisaki, S. Uchida, A. Fujimori, Z. Hussain, and Z.-X. Shen, Phys. Rev. Lett. **86**, 5578 (2001).
[81] H. Ding, J. R. Engelbrecht, Z. Wang, J. C. Campuzano, S.-C. Wang, H.-B. Yang, R. Rogan, T. Takahashi, K. Kadowaki, and D. G. Hinks, cond-mat/0006143 (unpublished).
[82] I. Martin, G. Ortiz, A. V. Balatsky, and A. R. Bishop, Int. J. Mod. Phys. B **14**, 3567 (2000).
[83] C. Bernhard, J. L. Tallon, Th. Blasius, A. Golnik, and Ch. Niedermayer, Phys. Rev. Lett. **86**, 1614 (2001).
[84] R. S. Markiewicz, cond-mat/0108075 (unpublished).
[85] R. S. Markiewicz, J. Phys.: Condens. Matter **2**, 665 (1990); A. Himeda and M. Ogata, Phys. Rev. Lett. **85**, 4345 (2000).
[86] M. R. Norman, Phys. Rev. B **61**, 14 751 (2000); Y.-J. Kao, Q. Si, and K. Levin, *ibid.* **61**, 11 898 (2000).